Journal of Solid State Chemistry 181 (2008) 2580–2585

Contents lists available at ScienceDirect

Journal of Solid State Chemistry

journal homepage: www.elsevier.com/locate/jssc

Solid solubility and phase transitions in the system $LaNb_{1-x}Ta_xO_4$

Fride Vullum, Fabian Nitsche, Sverre Magnus Selbach, Tor Grande *

Department of Materials Science and Engineering, Norwegian University of Science and Technology, Trondheim 7491, Norway

ARTICLE INFO

Article history:
Received 10 February 2008
Received in revised form
28 May 2008
Accepted 7 June 2008
Available online 19 June 2008

Keywords:
Phase transitions
Solid solutions
Ferroelasticity
$LaNbO_4$
$LaTaO_4$

ABSTRACT

The solid solubility between $LaNbO_4$ and $LaTaO_4$ was investigated by X-ray diffraction, and a two-phase region was observed in the composition region $LaNb_{1-x}Ta_xO_4$ where $0.4\leqslant x\leqslant 0.8$. Single-phase $LaNb_{1-x}Ta_xO_4$ $(0\leqslant x\leqslant 0.4)$ with the monoclinic Fergusonite structure at ambient temperature, was observed to transform to a tetragonal Scheelite structure by in-situ high-temperature X-ray diffraction, and the phase transition temperature was shown to increase with increasing Ta-content. This ferroelastic to paraelastic second-order phase transition was described by Landau theory using spontaneous strain as an order parameter. The thermal expansion of $LaNb_{1-x}Ta_xO_4$ $(0\leqslant x0.4)$ was shown to be significantly higher below the phase transition than above. Single-phase $LaNb_{1-x}Ta_xO_4$ $(0.8\leqslant x\leqslant 1)$ with another monoclinic crystal structure at ambient temperature was shown to transform to an orthorhombic crystal structure by X-ray diffraction and differential scanning calorimetry. The phase transition temperature was observed to decrease with decreasing Ta-content. Finally, orthorhombic $LaTaO_4$ could also be transformed to monoclinic $LaTaO_4$ at ambient temperature by applying a uniaxial pressure of 150–170 MPa, reflecting the lower molar volume of monoclinic $LaTaO_4$.

1. Introduction

$LaNbO_4$ with the monoclinic Fergusonite crystal structure at ambient temperature has been shown to possess ferroelastic properties, resulting in non-elastic behavior when exposed to mechanical stresses [1–4]. At elevated temperature $LaNbO_4$ transforms by a second-order phase transition to the tetragonal Scheelite structure [5]. The high-temperature tetragonal phase corresponds to the paraelastic state [4], and the phase transition has previously been shown to follow Landau theory using crystallographic strain as an order parameter [5]. The chemically related material $LaTaO_4$ is not isostructural with $LaNbO_4$ [6], and literature is not conclusive concerning the crystal structure at ambient conditions. A phase transition not far above room temperature has hampered the determination of the crystal structure at ambient temperature [6,7,11].

$LaNbO_4$ has also recently been reported by Haugsrud and Norby [8,9] as an electrolyte material candidate in solid oxide fuel cells due to its considerable proton conductivity at elevated temperatures. The proton conductivity is significantly lower than the state of the art oxide proton conductors based on alkali earth cerates and zirconates [10], but despite this fact $LaNbO_4$ has promising properties due to the expected higher thermodynamic stability of $LaNbO_4$ in $CO_2(g)$ and $H_2O(g)$ containing atmosphere [8]. In addition, Haugsrud and Norby [11] have reported considerable proton conductivity in $LaTaO_4$.

According to a previous study the thermal expansion of $LaNbO_4$ is strongly influenced by the ferroelastic to paraelastic phase transition [12], and it is therefore of interest to investigate the influence of the solid solution of $LaTaO_4$ in $LaNbO_4$ on the structural and thermal properties. Here, we report a study on the solid solubility of $LaTaO_4$ and $LaNbO_4$. The structural properties and phase transitions of the solid solutions have been analyzed by high-temperature X-ray diffraction and differential scanning calorimetry.

2. Experimental

Samples of $LaNb_{1-x}Ta_xO_4$ with seven different compositions ($x = 0.2$, 0.4, 0.5, 0.6, 0.7, 0.8, and 1) were obtained from the oxides La_2O_3 (Merck, 99.5%), Nb_2O_5 (Sigma-Aldrich, 99.9%), and Ta_2O_5 (Merck, 99%) through solid-state reaction synthesis. The starting oxides were dried at 600 °C for 6–10 h before weighing and mixing with a mortar and pestle. The homogeneously mixed powder was then uniaxially pressed into pellets at about 170 MPa and sintered two or three times at 1400 °C for 10 h, with intermediate grindings. Samples with higher Nb_2O_5 content generally required two cycles, while the Ta_2O_5 rich samples needed to be sintered a third time in order to obtain a phase-pure powder. Exceptions included the samples near the two-phase

---

* Corresponding author. Fax: +47 73 59 08 60.
E-mail address: tor.grande@material.ntnu.no (T. Grande).

0022-4596/$ - see front matter © 2008 Elsevier Inc. All rights reserved.
doi:10.1016/j.jssc.2008.06.032

boundaries, which required more than three annealing cycles to give phase-pure powders.

All the samples were characterized by X-ray diffraction (XRD) using a Bruker D8 Advance powder diffractometer (Våntec detector, Cu-$K\alpha$ radiation) for qualitative analysis at room temperature. High-temperature XRD (HTXRD) measurements for Rietveld refinements were performed with a Siemens D5005 $\theta-\theta$ diffractometer (Cu-$K\alpha$ radiation) with a secondary monochromator, while high-resolution diffractograms at room temperature were obtained using a Siemens D5005 $2\theta-\theta$ diffractometer (Cu-$K\alpha$ radiation) with a primary monochromator. Formation and structure of the monoclinic forms of $LaTaO_4$ and $LaNbO_4$, and the orthorhombic form of $LaTaO_4$ were confirmed via Rietveld refinement of diffraction data collected at room temperature and 300 °C, respectively, using structural models taken from Hartenbach et al. [6], Tsunekawa et al. [3], and Cava et al. [7]. For the high-temperature orthorhombic form of $LaTaO_4$ the x-position of the oxygen O(4) atom was fixed according to literature values [7] in order to compensate for the absence of a special position which fixes the origin in x. The evolution of the crystallographic cell parameters with temperature was determined via a Pawley-type full pattern fitting [13], with reflections from the Pt sample holder acting as an internal reference during the fitting procedure. All diffraction data analysis was performed using TOPAS software [14].

In addition to XRD analysis, two powder samples with the compositions $LaTaO_4$ and $LaNb_{0.2}Ta_{0.8}O_4$ were analyzed by differential scanning calorimetry (DSC). The analysis was performed with a Perkin Elmer DSC 7, PE Thermal Analysis Controller TAC 7/DX and Pyris v. 3.81 software. Samples of ~50 mg were encapsulated in aluminum sample pans and the measurements were done with 40 °C min^{-1} heating and cooling rates in the temperature region 25–550 °C.

3. Results and discussion

Room temperature XRD analysis of the different compositions showed that single-phase materials could be obtained for $x = 0$, 0.2, 0.4, 0.8, and 1. For the compositions where $x = 0.5$, 0.6, and 0.7 it was not possible to obtain phase-pure samples even after numerous cycles of sintering with intermediate grindings. The qualitative analysis revealed that the solid solubility limits exist somewhere between $LaNb_{0.6}Ta_{0.4}O_4$ and $LaNb_{0.5}Ta_{0.5}O_4$ on the Nb-rich side and between $LaNb_{0.3}Ta_{0.7}O_4$ and $LaNb_{0.2}Ta_{0.8}O_4$ on the Ta-rich side. For the Ta-rich samples, this is a larger range of solid solubility than reported previously by Arkhipova et al. [15].

The synthesis of $LaTaO_4$, resulting in only a single polymorph, proved to be more challenging than first expected. From XRD analysis of the powder two co-existing polymorphs could be observed at room temperature; a monoclinic phase and an orthorhombic phase. The amount of orthorhombic $LaTaO_4$ was increased by heating the sample as a powder in a range from 500 to 1400 °C. It is worth noting that annealing the sample as powder or pellet did have an effect on the result. If the powder was annealed to 1400 °C, the amount of the orthorhombic phase increased, while annealing a pellet favored the formation of the monoclinic phase. The monoclinic phase with lowest molar volume may be stabilized by internal stresses in the pellets due the crystallographic anisotropy of $LaTaO_4$. These stresses are not present in loose powders.

Attempts to prepare single-phase $LaTaO_4$ samples with the solid-state method at lower temperatures were unsuccessful. The phase ratio could however, be influenced by applying a uniaxial pressure of 150–170 MPa. These experiments were performed simply by pressing powder into a pellet at room temperature, followed by XRD analysis. This pressure treatment transformed the powder to phase-pure monoclinic $LaTaO_4$. Rietveld refinements performed on the X-ray diffractogram obtained from the pure monoclinic powder gave the structural parameters presented in Table 1, which are in accordance with values calculated by Hartenbach et al. [6] and Kurova et al. [18]. This powder was also investigated by HTXRD and DSC (see Figs. 1 and 2). From the DSC data a phase transition from monoclinic to orthorhombic was found to take place around 240 ± 5 °C upon heating. In Fig. 2 this is shown by the intersection of the slope of the endothermic peak with the base line. The HTXRD data recorded confirmed the phase transition from the monoclinic to the orthorhombic phase upon heating (see Fig. 1). The structural parameters for orthorhombic $LaTaO_4$, given in Table 2, were determined from Rietveld refinements of the X-ray diffractogram obtained above the phase transition temperature. These data agree with those previously found by Cava and Roth [7].

Of all the different compositions of $LaNb_{1-x}Ta_xO_4$ the Ta-rich powder with $x = 0.8$ was the most difficult sample to synthesize, needing as much as 4 cycles of annealing with intermediate grindings in order to obtain a phase-pure powder. This composition also exhibited a mixture of the monoclinic and orthorhombic polymorphs, and a pressure of 300–400 MPa was applied to the sample in order to obtain a monoclinic sample at room temperature. DSC measurements obtained for the monoclinic powder (see Fig. 3) demonstrated a phase transition from the monoclinic to the orthorhombic phase at 100 ± 5 °C, which is a considerable decrease in transition temperature compared to the corresponding temperature found for pure $LaTaO_4$. The reduction in transition temperature explains the higher tendency for $LaNb_{0.2}Ta_{0.8}O_4$ to sustain the orthorhombic form at ambient temperature. Unit cell parameters were calculated by performing Rietveld refinements on the XRD data obtained for the orthorhombic polymorph. These values are plotted in Fig. 4 together with the unit cell parameters found for the orthorhombic $LaTaO_4$ at 300 °C. It can be seen that a and c decrease with substitution of Nb for Ta, while b increases for the Nb-doped sample.

The apparent influence of pressure on the monoclinic to orthorhombic phase transformation of $LaTaO_4$ can be understood from thermodynamics. The molar volume of the monoclinic phase is lower than for the orthorhombic, giving $\Delta V > 0$ for the phase transition. The corresponding entropy change for the phase transition is also positive as shown by DSC. According to the Clausius–Clapeyron equation, $dT/dP = \Delta V/\Delta S$, the slope of the temperature vs pressure for the phase transition is positive. Pressure will therefore stabilize the monoclinic polymorph relative to the orthorhombic.

Synthesis of phase-pure $LaNb_{1-x}Ta_xO_4$ for $x = 0$, 0.2, 0.4 was not as challenging as obtaining phase-pure samples of the Ta-rich powders. However, close to the solubility limit, the samples

Table 1
Cell parameters and atom positions for monoclinic $LaTaO_4$

Space group: $P2_1/c$			
a (Å)	b (Å)	c (Å)	β (deg)
7.6281(81)	5.5781(02)	7.8203(71)	101.533(80)
Atom	x	y	z
La	0.3412(71)	0.7743(94)	0.0964(42)
Ta	0.1686(61)	0.2644(74)	0.3007(22)
O(1)	0.1706(19)	0.1713(27)	0.0618(24)
O(2)	0.0507(23)	0.5779(29)	0.2104(22)
O(3)	0.3783(20)	0.4843(29)	0.3245(21)
O(4)	0.3352(19)	0.9947(30)	0.3592(20)

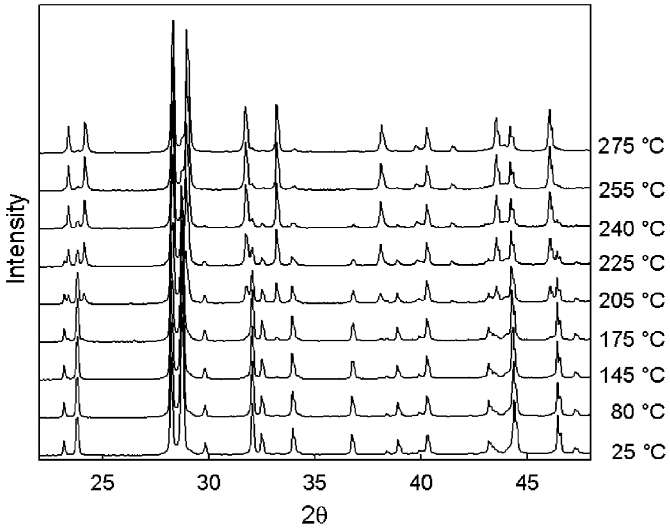

Fig. 1. High-temperature XRD for $LaTaO_4$.

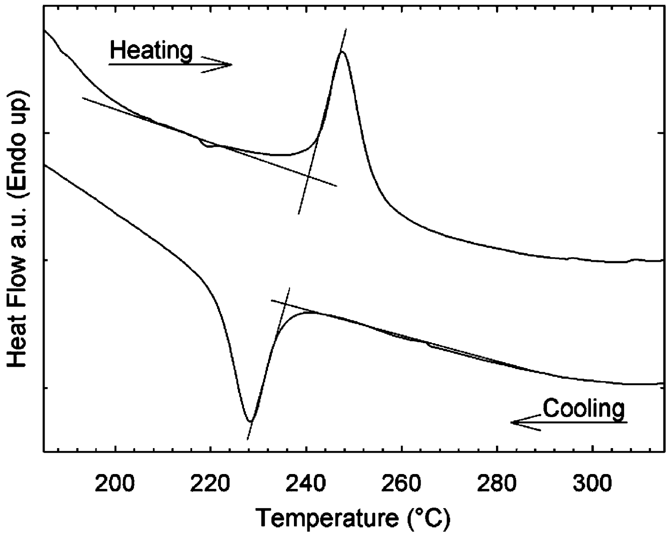

Fig. 2. DSC measurements for $LaTaO_4$.

Table 2
Cell parameters and atom positions for orthorhombic $LaTaO_4$

Space group: $A2_1am$			
a (Å)	b (Å)	c (Å)	β (deg)
5.6415(82)	14.719(51)	3.9404(41)	90
Atom	x	y	z
La	0.171(28)	0.1682(24)	0
Ta	0.212(30)	0.4144(24)	0
O(1)	0.422(32)	0.3077(54)	0
O(2)	0.949(42)	0.3381(55)	0
O(3)	0.563(18)	0.4724(75)	0
O(4)	0.2496	0.9055(51)	0

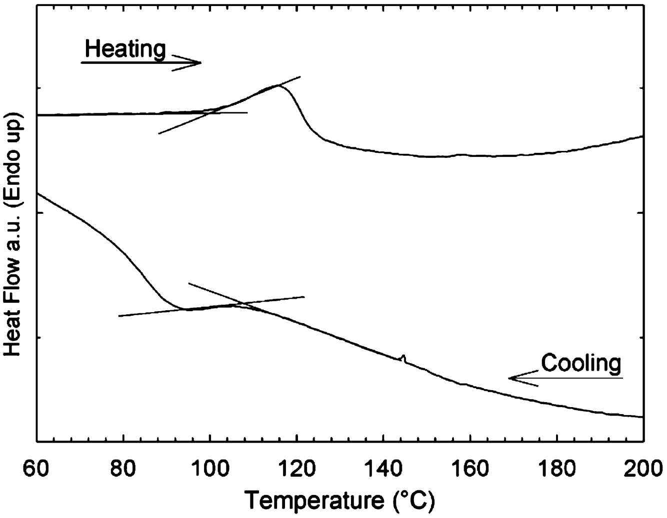

Fig. 3. DSC measurements for $LaNb_{0.2}Ta_{0.8}O_4$.

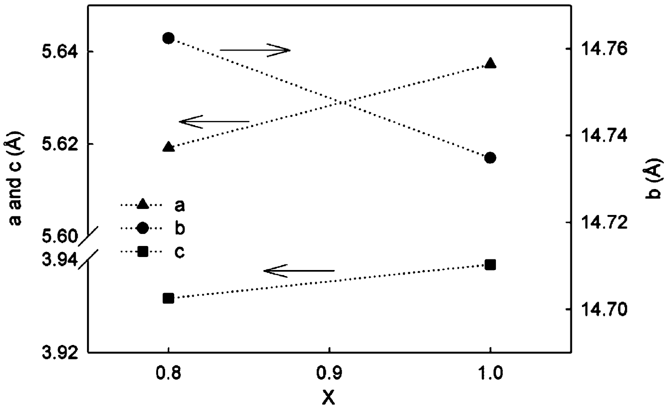

Fig. 4. Cell parameters for orthorhombic $LaTaO_4$ doped with Nb.

Table 3
Cell parameters and atom positions for monoclinic $LaNbO_4$

Space group: $I2/a$			
a (Å)	b (Å)	c (Å)	β (deg)
5.5626(02)	11.519(61)	5.2013(06)	94.06(89)
Atom	x	y	z
La	0	0.6304(33)	0.25
Nb	0	0.1047(83)	0.25
O(1)	0.2265(31)	0.378(13)	0.0497(30)
O(2)	0.1424(34)	0.2089(13)	0.4827(22)

needed an extra cycle of regrinding and heating in order to become phase pure. Rietveld refinements were performed on the pure $LaNbO_4$ and the cell parameters and atom positions found are presented in Table 3. These values are in agreement with values calculated by Tsunekawa et al. [3]. In addition, Pawley-type full pattern fitting was performed on $LaNbO_4$ as well as the Ta-doped samples ($x = 0.2$, 0.4), and Fig. 5 shows the results obtained for the calculated and recorded X-ray diffraction patterns of $LaNb_{0.6}Ta_{0.4}O_4$ at room temperature, with the difference indicated in gray. The evolution of the room temperature cell parameters of *m*-phase with increasing Ta-content for the three Nb-rich samples is shown in Fig. 6a. Parameters *b* and *c* both decrease with increasing Ta-content, while *a* increases

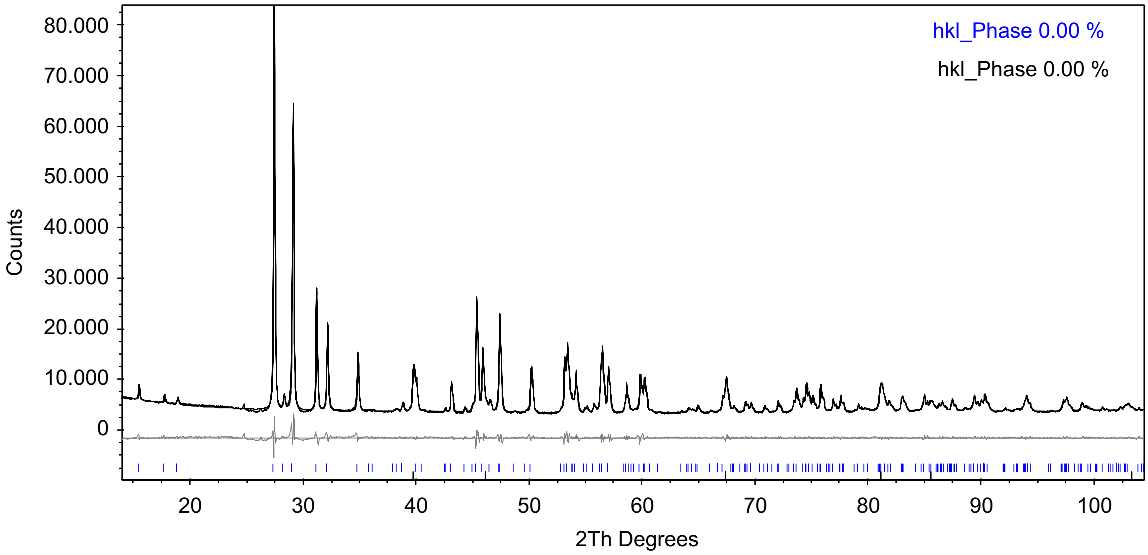

Fig. 5. Calculated and recorded X-ray diffraction patterns for $LaNb_{0.6}Ta_{0.4}O_4$ at room temperature, from TOPAS.

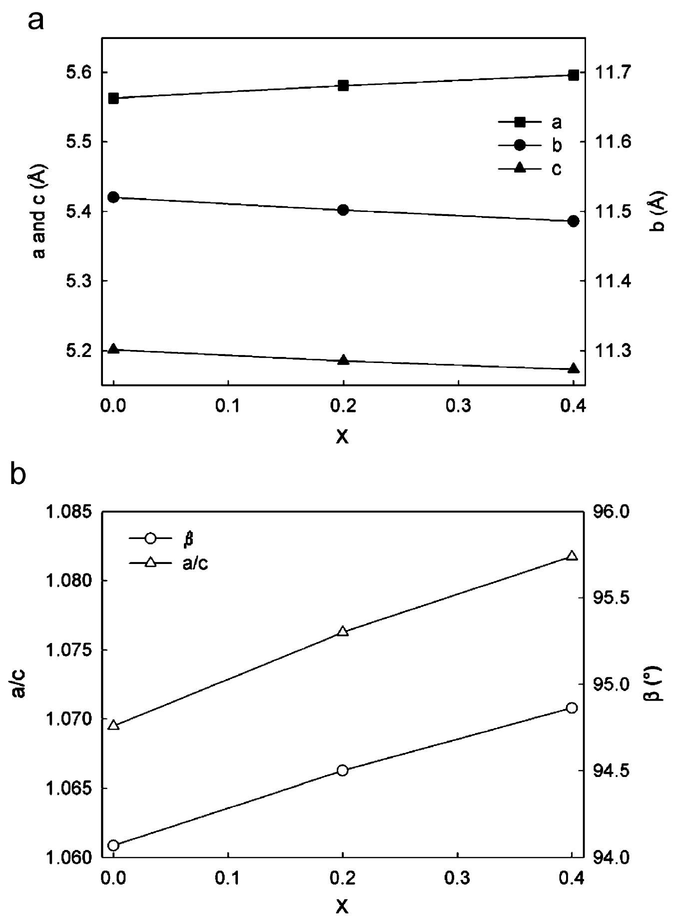

Fig. 6. (a) Cell parameter evolution as a function of Ta-doping in the solid solution $LaNb_{1-x}Ta_xO4$ and (b) deviation from tetragonality.

accordingly. The change with composition of the monoclinic angle β, and the ratio between a and c are shown in Fig. 6b and are expressions of the deviation of the crystal structure from tetragonality. If the structure was to go through a monoclinic to tetragonal phase transition, the a/c ratio would have to approach unity and finally be equal to one, while b would approach 90° for the tetragonal polymorph. Here however, it is clear that both values are increasing, moving away from the required parameter values, and the crystal structure will therefore never become tetragonal at ambient conditions with increasing Ta-doping.

In addition to room temperature XRD, HTXRD was performed on the Nb-rich compositions. For the purpose of unit cell refinements in TOPAS, data was recorded from room temperature to 1000 °C for a 2θ range of 14–105° in order to give accurate data and increase the quality of the refinement. The results can be seen in Fig. 7a and b. The cell parameter a decreases with increasing temperature for all compositions, while c increases (Fig. 7a). Both parameters are approaching the same value as the temperature nears the phase transition. The phase transition temperature can also be estimated from the monoclinic angle β which decreases with temperature for all three compositions and approaches 90° nearing the phase transition. Data from Prytz and Tafto [16] on $LaNbO_4$ are included as a reference in both Fig. 7a and b, showing that our data is in good agreement with literature values. Cell parameters as functions of temperature have also been calculated by Jian and Wyman [5]. However, their results show considerable deviation from our data and are therefore not included here.

The phase transition from monoclinic to tetragonal for $LaNbO_4$ has previously been found to occur at a temperature in the range of 490–525 °C [3–5], which is consistent with the results obtained here. From the evolution of the cell parameters a, c, and β it can be seen that this transition temperature is increased by substituting tantalum for niobium. The transition temperatures found for the three compositions are summarized in Table 4. The development towards higher transition temperature with increasing Ta-content can be explained from structural considerations. Nb is tetrahedrally coordinated in the high-temperature tetragonal phase, but exhibits an increase in coordination number to 4+2 in the monoclinic phase, approaching an octahedral coordination. The Ta-ion in $LaTaO_4$ has a coordination number of 6, and the substituted Ta-ions in $LaNb_{1-x}Ta_xO_4$ will facilitate the progression of the Nb-ion site towards an octahedral coordination, which stabilizes the low-temperature phase and thereby increases the transition temperature.

It has been suggested previously by Jian and Wyman [5] that the temperature induced monoclinic to tetragonal phase

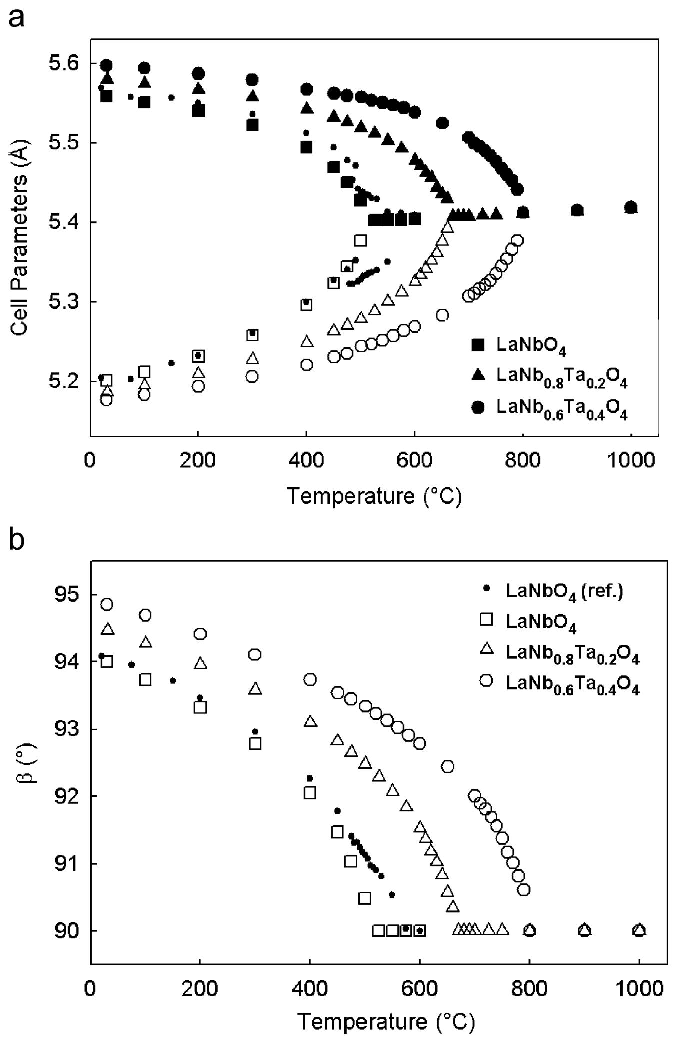

Fig. 7. (a) Evolution of cell parameters *a* and *c* for $LaNb_{1-x}Ta_xO_4$ ($x = 0, 0.2, 0.4$), where *a* is denoted by closed symbols and *c* by open symbols. (b) Evolution of the monoclinic angle β with increasing temperature for the same compositions. In both (a) and (b) reference data for $LaNbO_4$ is included [16] and are shown as small dots.

Table 4
Thermal expansion coefficients (TEC) and transition temperatures (T_c) for $LaNb_{1-x}Ta_xO_4$

	TEC monoclinic ($10^{-6}\,°C^{-1}$)	TEC tetragonal ($10^{-6}\,°C^{-1}$)	T_c (°C)
$LaNbO_4$	17.3 ± 0.5	7.1 ± 0.7 9	510 ± 10
$LaNb_{0.8}Ta_{0.2}O_4$	15.7 ± 0.3	9.1 ± 0.1	670 ± 10
$LaNb_{0.6}Ta_{0.4}O_4$	14.0 ± 0.2	11.5 ± 1	800 ± 10

transition in $LaNbO_4$ is second order in nature. This was supported by calculating the spontaneous strain (e_s) and comparing the relationship between the magnitude of e_s and the order parameter (η) in Landau's theory. For a second-order phase transition the order parameter should have the form

$$\eta = \left[\frac{T_{trs} - T}{T_{trs}}\right]^{1/2} \qquad (1)$$

where T_{trs} is the phase transformation temperature. In the $LaNbO_4$ system the order parameter and the spontaneous strain are proportional to each other and a linear relationship can be found by comparing e_s and η, giving the following equation:

$$\eta = k e_s \qquad (2)$$

where *k* is constant for all temperatures and specific to the system in consideration. The equations used to calculate the strain components are adopted from Schlenker et al. [17], and the relationship between the order parameter and the magnitude of the spontaneous strain is plotted in Fig. 8. The open symbols show the calculated values for e_s, while the solid lines indicate the order parameter divided by *k* (η/k), where *k* is given by 10.8, 10.0, and 9.1 for $x = 0$, 0.2, and 0.4, respectively. At low temperatures there is some deviation from the linear relationship. However, close to the phase transformation temperature good agreement is seen between e_s and η, demonstrating that a second-order transformation occurs for all three compositions.

The normalized volume changes as a function of temperature for all three of the Nb-rich compositions were estimated and plotted (not shown here). From a linear approximation to these curves the monoclinic and tetragonal linear thermal expansion coefficients (TEC) were calculated, and these are presented in Table 4. TEC found for pure $LaNbO_4$ are slightly higher than what has been reported previously by Mokkelbost et al. [12], but still within acceptable range. An interesting observation here is the decrease in the monoclinic TEC with increasing Ta-substitution,

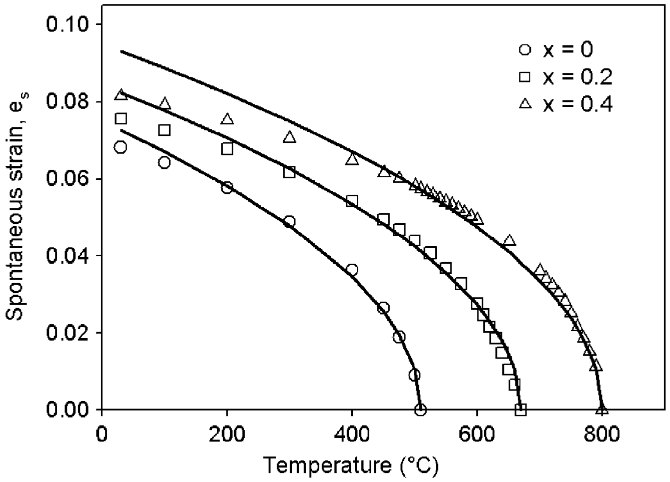

Fig. 8. Relationship between the order parameter and the magnitude of the spontaneous strain. Symbols show the calculated spontaneous strain (e_s), while the solid lines indicate the order parameter divided by *k* (η/k). For $x = 0$, 0.2, and 0.4 the constant *k* is found to be 10.8, 10.0, and 9.1, respectively.

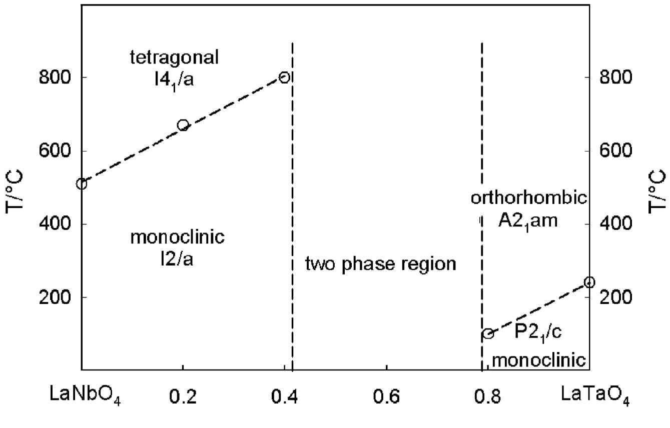

Fig. 9. Phase diagram for the binary system $LaNbO_4$–$LaTaO_4$.

while the tetragonal TEC increases accordingly. At 40% Ta-substitution the monoclinic and tetragonal thermal expansion coefficients only differ by a value of approximately $2.5 \times 10^{-6}\,^{\circ}C^{-1}$, compared to four times that value for pure $LaNbO_4$.

In an attempt to summarize the data collected in this study, a tentative phase diagram for the solid solution $LaNb_{1-x}Ta_xO_4$ has been sketched and is shown in Fig. 9. The vertical dashed lines indicate the compositional limits between the two-phase and single-phase regions, while the sloped dashed lines show the development of the temperature-induced phase transitions with varying composition. The measured phase transition temperatures are shown by circles.

4. Conclusion

The solid solution $LaNb_{1-x}Ta_xO_4$ forms a single-phase material for $x \leqslant 0.4$ and $x \geqslant 0.8$, while all other values of x form a two-phase material. Synthesis of phase-pure $LaTaO_4$ was challenging and proved to be very sensitive to annealing temperatures and pressure applied to already sintered powder, giving a mixture of the orthorhombic and monoclinic polymorphs for most synthesis conditions. Cell parameters and atom positions were calculated for the phase-pure powders. For $LaTaO_4$ a phase transition from monoclinic to orthorhombic was found to occur at $240 \pm 5\,^{\circ}C$, with a decrease in transition temperature to $100 \pm 5\,^{\circ}C$ when doped with 20% niobium.

For $LaNbO_4$ a second-order phase transition from a room temperature monoclinic to a high-temperature tetragonal polymorph was found to occur at $510 \pm 10\,^{\circ}C$. The phase transitions for $LaNb_{0.8}Ta_{0.2}O_4$ and $LaNb_{0.6}Ta_{0.4}O_4$ were also found to be second order in nature, with the transition temperature increasing with increasing tantalum content. The monoclinic linear thermal expansion coefficients (TEC) for the three Nb-rich compositions decrease with increasing tantalum content, while the tetragonal TEC increase accordingly. This significant reduction in the difference between the monoclinic and tetragonal TEC may contribute to make the material a more interesting candidate as an electrolyte for thin-film solid oxide fuel cells by easing the processing of the material.

Acknowledgment

Work was supported by NTNU, the Gas Technology Center at NTNU and The Research Council of Norway.

References

[1] T. Takagi, Y.H. Choa, T. Sekino, K. Niihara, Key Eng. Mater. 2 (1999) 181.
[2] S. Tsunekawa, A. Kasuya, Y. Nishina, T. Fukuda, Mater. Trans. JIM 37 (4) (1996) 650.
[3] S. Tsunekawa, T. Kamiyama, K. Sasaki, H. Asano, T. Fukuda, Acta Crystallogr. A 49 (1993) 595.
[4] W.I.F. David, Mater. Res. Bull. 18 (1983) 749.
[5] L. Jian, C.M. Wayman, J. Am. Ceram. Soc. 80 (1997) 803.
[6] I. Hartenbach, F. Lissner, T. Nikelski, S.F. Meier, H. Muller-Bunz, T. Schleid, Z. Anorg. Allg. Chem. 631 (2005) 2377.
[7] R.J. Cava, R.S. Roth, J. Solid State Chem. 36 (1981) 139.
[8] R. Haugsrud, T. Norby, Solid State Ion. 177 (2006) 1129.
[9] R. Haugsrud, T. Norby, Nat. Mater. 5 (2006) 193.
[10] K.D. Kreuer, S. Adams, W. Munch, A. Fuchs, U. Klock, J. Maier, Solid State Ion. 14 (2001) 295.
[11] R. Haugsrud, T. Norby, J. Am. Ceram. Soc 90 (2007) 1116.
[12] T. Mokkelbost, Ph.D. Thesis, Norwegian University of Science and Technology, Trondheim, Norway, 2006.
[13] G.S. Pawley, J. Appl. Cryst. 14 (1981) 357.
[14] Bruker AXS: TOPAS V2.1: General Profile and Structure Analysis Software for Powder Diffraction Data, Bruker AXS, Karlsruhe, Germany, 2003.
[15] E.V. Arkhipova, M.G. Zuev, L.V. Zolotukhina, J. Alloys Compds. 305 (2000) 58.
[16] O. Prytz, J. Tafto, Acta Mater. 53 (2005) 297.
[17] J.L. Schlenker, G.V. Gibbs, M.B. Boisen, Acta Crystallogr. A 34 (1978) 52.
[18] T.A. Kurova, V.B. Aleksandrov, Dokl. Akad. Nauk SSSR 201 (1971) 1095.